Article

PGS/Gelatin Nanocomposite Electrospun Wound Dressing

Mahyar Naseri , Aysan Hedayatnazari , Lobat Tayebi *

Posted Date: 8 May 2023

doi: 10.20944/preprints202305.0451.v1

Keywords: Electrospun wound dressing; Skin tissue engineering; Regenerative medicine; Gelatin; Poly (glycerol sebacate); Diabetic wound

Article

PGS/Gelatin Nanocomposite Electrospun Wound Dressing

Mahyar Naseri [1], Aysan Hedayatnazari [2] and Lobat Tayebi [1,*]

[1] Marquette University School of Dentistry, Milwaukee, Wisconsin 53233, United States
[2] Department of Biomedical Engineering, Medical College of Wisconsin & Marquette University, Milwaukee, Wisconsin, USA
* Correspondence: lobat.tayebi@marquuett.edu, Marquette University School of Dentistry, Milwaukee, Wisconsin 53233, United States

Abstract: Infectious diabetic wounds can result in severe injuries or even death. Biocompatible wound dressings offer one of the best ways to treat these wounds, but creating a dressing with suitable hydrophilicity and biodegradation rate can be challenging. To address this issue, we used the electrospinning method to create a wound dressing composed of poly(glycerol sebacate) (PGS) and gelatin (Gel). We dissolved the PGS and Gel in acetic acid (75 v/v%) and added EDC/NHS solution as a crosslinking agent. Our measurements revealed that the scaffolds' fiber diameter ranged from 180.2 to 370.6 nm, and all the scaffolds had porosity percentages above 70%, making them suitable for wound healing applications. Additionally, we observed a significant decrease ($p < 0.05$) in the contact angle from 110.8° ± 4.3° for PGS to 54.9° ± 2.1° for PGS/Gel scaffolds, indicating an improvement in hydrophilicity of the blend scaffold. Furthermore, our cell viability evaluations demonstrated a significant increase ($p < 0.05$) in cultured cell growth and proliferation on the scaffolds during the culture time. Our findings suggest that the PGS/Gel scaffold has potential for wound healing applications.

Keywords: electrospun wound dressing; skin tissue engineering; regenerative medicine; gelatin; Poly (glycerol sebacate); diabetic wound

1. Introduction

Skin is the body's largest organ, with multiple critical functions. It serves as a protective barrier against harmful microorganisms and mechanical damage, helps maintain the body's temperature balance, and aids in the excretion of waste products [1–5]. The integrity of the skin is affected by burns, trauma, and diabetes which can lead to skin inflammation and bacterial infection.

Wounds, caused by a lack of skin integrity, are a major issue in the world, and have caused economic and social problems in all societies [6–8]. The human skin has the ability to regenerate itself against small and superficial wounds. However, in the case of severe and deep wounds, the natural healing process is not enough, and protection of the injured area is needed until the wound is completely healed. Therefore, the fabrication of proper wound dressing to accelerate the wound healing process is necessary [9]. The ideal wound dressing should perform tasks such as providing a moist environment around the wound, exchanging gas and nutrients, collecting exudate from the wound site, not adhering to the wound, and to prevent bacterial infection and allergic reactions. Accordingly, a wound dressing should be biocompatible, biodegradable, swellable, elastic, and antibacterial. In addition, having a porous structure is necessary for a dressing to improve cell growth, proliferation, migration, and angiogenesis. As a result, the fabrication of an ideal wound dressing to have all these items require great effort and precision [10,11].

There are various methods, such as solvent casting [12], salt leaching [13], freeze-drying [14], and electrospinning [15] in the fabrication of wound dressings. Electrospinning is an effective technique that can use a wide variety of biomaterials to produce nanofibrous structures with uniform

 doi:10.20944/preprints202305.0451.v1

and continuous nanofibers and high specific surface area. This method fabricates highly porous structures, which simplify gas and nutrient exchange and provide moisture around the wound, preventing excessive drying of the wound. Also, electrospun nanofibers have similar flexibility and tensile strength as human skin and can simulate the extracellular matrix (ECM) structure of the skin tissue, providing a microenvironment which promotes cell attachment, growth, and proliferation [16–18]. Hadizadeh et al. [19] fabricated a poly (ε-caprolactone) (PCL)/gelatin (Gel)-based electrospun scaffold, incorporated with surfactin (Sur) and curcumin (Cur). The PCL/0.2Sur-Gel/3%Cur scaffold showed suitable wettability, mechanical properties, degradation rate, antibacterial activity, and biological properties (*in vitro* and *in vivo*). Also, Bao et al. [20] fabricated an electrospun scaffold composed of hyaluronic acid (HA), graphene (Gr), and polyphenolic tannic acid (TA). The in vivo results indicated that after 14 days, the wound area of the scaffold loaded with 0.3 w/v% TA was 1.12 ± 0.54 mm^2, was significantly ($p < 0.05$) better than that of the HA and control groups. However, in addition to the fabrication method of the scaffolds, the biomaterials used for fabricating the scaffolds also have a significant effect on their final properties.

Poly (glycerol sebacate) (PGS) is a tough polyester which is synthesized by polycondensation of glycerol and sebacic acid. It is a biocompatible, elastic, and biodegradable polyester, and its degradation products can be removed by the body's metabolism. However, this polymer does not have the ideal hydrophilicity and degradation rate and cannot form a nanofibrous structure due to its low spinnability [21–23]. Thus, it should be blended with hydrophilic polymers.

Gelatin (Gel) is a naturally occurring hydrophilic polymer that can be extracted from collagen, the most abundant protein of the extracellular matrix (ECM). Gel offers several advantages, including biocompatibility, non-immunogenicity, and biodegradability, making it a suitable material for supporting cell attachment, growth, and proliferation. Moreover, Gel is readily available at a relatively low cost. It can be electrospun using aqueous solutions of acetic acid, formic acid, or ethanol. [24,25]. In a study, Farahani et al. [26] fabricated a cellulose acetate/gelatin/*Zataria multiflora* nanoemulsion (CA/Gel/*ZM*-nano) wound dressing using the electrospinning method. The results showed that adding Gel decreased the rate of drug release and increased the cell viability of the dressing. Also, in another study, Sanhueza et al. [25] prepared an electrospun scaffold composed of Gel/poly-3-hydroxybutyrate (PHB) nano/microfibers for the healing of diabetic wounds. In vivo results showed that for 14 days, the wound area decreased significantly ($p < 0.1$) after adding Gel to the scaffolds. Moreover, the histological analysis indicated that hypodermis was formed after treatment of the wounds with the Gel-PHB scaffold.

In this paper, we fabricated and evaluated a PGS/Gel nanofibrous structure using electrospinning to assess its morphological, physical, and biological properties. To the best of our knowledge, this study is the first to examine the fabrication and characterization of a PGS/Gel electrospun scaffold for wound healing applications. Our findings can provide valuable insights for biomedical engineers seeking to develop superior wound dressings with optimal properties.

2. Materials and Methods

2.1. Materials

The applied materials in this study have been shown in Table 1.

Table 1. Applied materials in this study.

Row	Material name	Company/Country made
1	Gelatin (Gel)	Sigma Aldrich/USA
2	Sebacic acid	Sigma Aldrich/USA
3	Glycerol	Sigma Aldrich/USA
4	N-Hydroxysuccinimide (NHS)	Merck/Germany
5	1-Ethyl-3-(3-dimethylaminopropyl) carbodiimide (EDC)	Merck/Germany
6	Acetic acid	Merck/Germany

Preprints (www.preprints.org) | NOT PEER-REVIEWED | Posted: 8 May 2023 doi:10.20944/preprints202305.0451.v1

7	Ethanol solution	Nasr/Iran
8	Phosphate-buffered saline (PBS)	GIBCO/USA
9	Human Dermal Fibroblasts (HDF) cell line	Cell Bank of Pasteur Institute/Iran
10	Dulbecco's modified eagle's medium (DMEM), Glutamax (High Glucose)	GIBCO/USA
11	Fetal bovine serum (FBS)	Vivacell/Iran
12	Penicillin/streptomycin	GIBCO/USA
13	Trypsin-EDTA (0.05% Trypsin in 0.04 mM EDTA)	Bioidea/Iran
14	Glutaraldehyde (25% Aqueous Solution)	Merck/Germany
15	Dimethyl sulfoxide (DMSO)	Sigma Aldrich/USA
16	3-(4,5-dimethylthiazol-2-yl)-2,5-diphenyltetrazolium bromide (MTT)	Sigma Aldrich/USA

2.2. Synthesis of poly (glycerol sebacate) (PGS) prepolymer

Based on the method presented by Kharaziha et al. [27] for synthesizing PGS prepolymer, firstly, a glycerin bath was prepared at 130 °C in a glass container, which had been placed on a magnetic stirrer equipped with a heating system (IKI/Germany). Then, glycerol, which had been degassed under a nitrogen atmosphere and at 130 °C for 2 h, was added to a three-necked flask placed in this bath. After the temperature of glycerol reached the temperature of the bath, sebacic acid powder, which had been dried at 55 °C in a vacuum oven (Memmert/Germany), was introduced to glycerol with a molar ratio of 1:1. This system was stirred on a magnetic stirrer under a slow flow of nitrogen gas and at 130 °C for 24 h. After the mentioned period and the cooling of the system, a paste-like material was obtained, which was the PGS prepolymer. The schematic of the synthesis process has been shown in Figure 1.

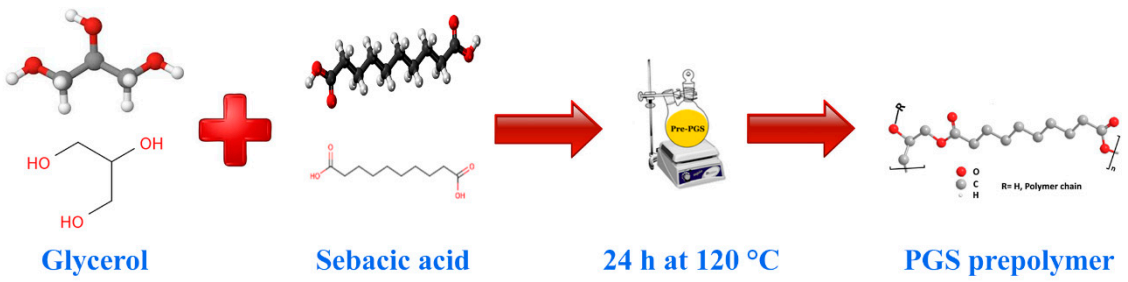

Figure 1. The schematic of the synthesis process of PGS prepolymer.

2.3. Fabrication of the electrospun scaffolds

Firstly, the PGS/Gel solution with a ratio of 3:1 was prepared using acetic acid 75 v/v% at 38-42 °C, and the final polymer concentration was set in the range of 10-30 wt. %. As a crosslinking agent, EDC/NHS was dissolved in ethanol and then introduced to the polymeric solution, followed by stirring for 30 min to complete the cross-linking process. Finally, all the samples were loaded in a 1-ml plastic syringe with a 21-gauge needle and electrospun using an electrospinning device (GMS300/Iran), and the concentration of the solution was optimized according to the solution spinnability and the quality of the nanofibers electrospun on laboratory slides. The electrospinning process was carried out at 25 °C. The prepared optimum scaffold was placed in a vacuum oven (Memmert/Germany) at room temperature for 6 h.

2.4. Morphological assessment

To assess the structural features of the scaffolds, such as morphology, porosity, and integrity, scanning electron microscopy (SEM, Seron AIS 2300C/Korea) was used. After cutting the scaffolds into the 1×1 cm^2 squares, they were fixed on a grid, followed by coating their surface with gold. Using

 doi:10.20944/preprints202305.0451.v1

SEM micrographs of the scaffolds, the diameter of 100 fibers was measured with Image J software (Wayne Rasband, National Institute of Health/USA), and the range of fiber diameter was determined [28]. Also, MATLAB (R2017b) software was applied to calculate the porosity of the scaffolds from their SEM micrographs [29].

2.5. Fourier transform infrared spectrometry

To evaluate the possible interactions between the two polymers and the chemical structure of the scaffolds, the Fourier transform infrared spectrometry (FTIR, JASCO FT/IR-6300/Japan) test was applied. The test was performed over a wavenumber range between 400 to 4000 cm^{-1} at room temperature.

2.6. Measurement of contact angle

Using a contact angle meter (XCA-50, PMC/Iran), the measurement of water contact angle (WCA) was applied to assess the hydrophilicity of all the scaffolds. The analysis was carried out at room temperature, and the sessile drop technique was used to record the contact angle. The droplet volume was set at 4 µl, and the measurements were performed after 15 s of dropping distilled water on the surface of the scaffolds.

2.7. In vitro degradation

Based on the ASTM F1635 standard, an in vitro degradation test was conducted to study the degradation rate of the scaffolds. In this regard, the samples were cut into 1×1 cm^2, and after weighing (W_0) them with a laboratory scale of 5 decimal places (PLS510-3A/Germany), they were immersed in 5 ml of phosphate buffer saline (PBS) solution, followed by incubation (Memmert/Germany) at 37 °C. On days 1, 4, 7, 14, and 21 of the incubation period, the samples were removed from the solution, rinsed with distilled water to remove the formed salts, and dried in a vacuum oven (Memmert/Germany) at 37 °C for 2 h before weighing (W_t), and the following formula was used to calculate the weight loss percentage:

$$\text{Weight loss\%} = \frac{W_0 - W_t}{W_0} \quad (1)$$

To avoid the effects of the degradation products on the quality of the solution that may affect the weight loss profile of the samples, the buffer solution was completely replaced every 24 h.

2.8. In vitro cellular studies

After cutting the scaffolds into circles with a diameter of 1.5 cm and sterilizing them with UV light, ethanol, and PBS, respectively, they were fixed in the wells of 24-well plates and prepared for cell seeding. The prepared human dermal fibroblast (HDF) cells were transferred to the flasks containing DMEM culture medium, which was supplemented with 10% FBS and 1% penicillin-streptomycin, and the flasks were kept in an incubator (Memmert/Germany) with 5% CO_2 at 37 °C for 3 weeks. Until the cell confluency reached 80%, the culture medium was renewed every 2 days. Then, the cells were trypsinized, and after counting the cells, 5×10^3 cells were seeded on the prepared scaffolds, followed by incubating the plates. The culture medium was renewed every other day until the end of the cell culture period.

According to the ISO-10993-5 standard, the MTT assay was applied to evaluate the viability of the cultured cells on the scaffolds, and the results were compared to the scaffold-free control sample. On the 3rd and 5th days of cell culture, the culture medium was removed, and the cells were rinsed twice with the PBS solution to remove the dead cells. Next, 200 µl of serum-free culture medium containing 20 µl of the MTT solution (5 mg/ml) was added to each well. After 4 h of incubation at 37 °C and 5% CO_2, the insoluble blue crystals of formazan were formed due to the presence of mitochondrial enzymes in living cells, and the color of the medium turned from yellow to dark blue. To dissolve the formazan crystals, 200 µl of DMSO solution was replaced with the MTT solution, and the pipetting process was performed for the complete dissolution of the crystals. Finally, the

 doi:10.20944/preprints202305.0451.v1

formazan solution was transferred to a 96-well plate, and the absorbance at the wavelength of 570 nm was measured with a microplate reader (BioTek-FLx800/USA).

The cells were cultured on the prepared scaffolds for up to 5 days to observe cell attachment and proliferation. After removing the culture medium on the 5th day of incubation, the samples were rinsed 3 times with the PBS solution, and 4% glutaraldehyde was applied to fix the cells, followed by keeping the samples at 4 °C for 2h. After that, the scaffolds were dehydrated using ethanol solution with concentrations of 50, 70, 80, 90, and 100 v/v%, respectively. After drying the scaffolds at room temperature, cell attachment and proliferation were assessed using SEM (Seron AIS 2300C/Korea) analysis.

2.9. Statistical analysis

Using SPSS software (n = 3; version 22) for statistical analysis, the data was evaluated via one-way ANOVA. The results (n = 3) were reported as mean ± standard deviation (SD). The significance level was defined where the *p*-value is less than 0.05 ($p < 0.05$).

3. Results

3.1. Optimization of electrospinning parameters

The effective parameters in the fabrication of polymer-based fibers via the electrospinning method, which influence the surface morphology and diameter of the fibers, can be divided into two categories: solution parameters and process parameters. Some examples of the solution parameters are solution viscosity and concentration, solvent volatility, and molecular weight of polymers. Among the process parameters, applied voltage, needle-to-collector distance, and solution flow rate can be mentioned. According to the results obtained from the experiments, it has been observed that in polymer concentrations less than 30 wt. %, electrospinning does not take place, and large drops of the solution have been sprayed on the collector. In polymer concentrations higher than 30 wt. %, only short, irregular, and thick fibers have been electrospun on the collector plate. Also, no spinning has been observed in PGS/Gel ratios of 2:1 and 1:1. In the polymer ratio of 2:1, only irregular fibers have been observed at a voltage above 25 kV, while the polymer ratio of 3:1 has resulted in regular and uniform fibers. As a result, in this research, the polymer concentration of 30 wt. % with a PGS/Gel ratio of 3:1 has been considered suitable. Other optimal electrospinning parameters are needle-to-collector distance = 15 cm, voltage = 20 kV, and flow rate = 0.5 ml/h.

3.2. Morphological assessment

The morphological properties of the scaffolds were investigated by SEM analysis (Figure 2). In the micrographs of the electrospun samples, a bead-less and porous structure of nanofibers can be observed. However, the distribution of fiber diameter in the sample containing gelatin, which has an average fiber diameter of 252.4 ± 32.5 nm, is more uniform than in the sample without it. Also, the results of analyzing SEM micrographs with MATLAB software show that the percentage of porosity in all the samples is above 75%. The results of the average fiber diameter and porosity percentage of the samples have been reported in Table 2.

Table 2. The average fiber diameter and porosity percentage of the samples.

Sample	Mean fiber diameter (nm)	Porosity percentage (%)
PGS	371.2 ± 64.8	77.2 ± 2.4
PGS/Gel	252.4 ± 32.5	80.8 ± 1.1

Preprints (www.preprints.org) | NOT PEER-REVIEWED | Posted: 8 May 2023 doi:10.20944/preprints202305.0451.v1

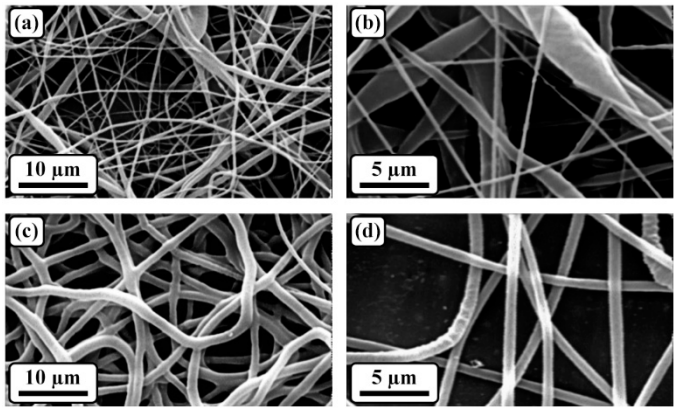

Figure 2. The SEM micrographs of (a and b) PGS and (c and d) PGS/Gel.

3.3. Structural evaluation

As shown in Figure 3a, the two peaks at 2933 and 2855 cm^{-1} are attributed to the presence of (CH_2) in the polymer chains. Also, the peaks at 1735 and 1177 cm^{-1} indicate the formation of C=O and C-O bonds, respectively, confirming the successful synthesis of PGS [30,31]. The analysis of the FTIR spectrum in Figure 3b shows the presence of gelatin amide bond peaks at wavenumbers of 1533 and 1637 cm^{-1} [32]. Also, the peak corresponding to the carbonyl group (C=O) shifted to 1728 cm^{-1}. In addition, the broad band in the range of 3100-3600 cm^{-1} is ascribed to the OH^- functional group [31].

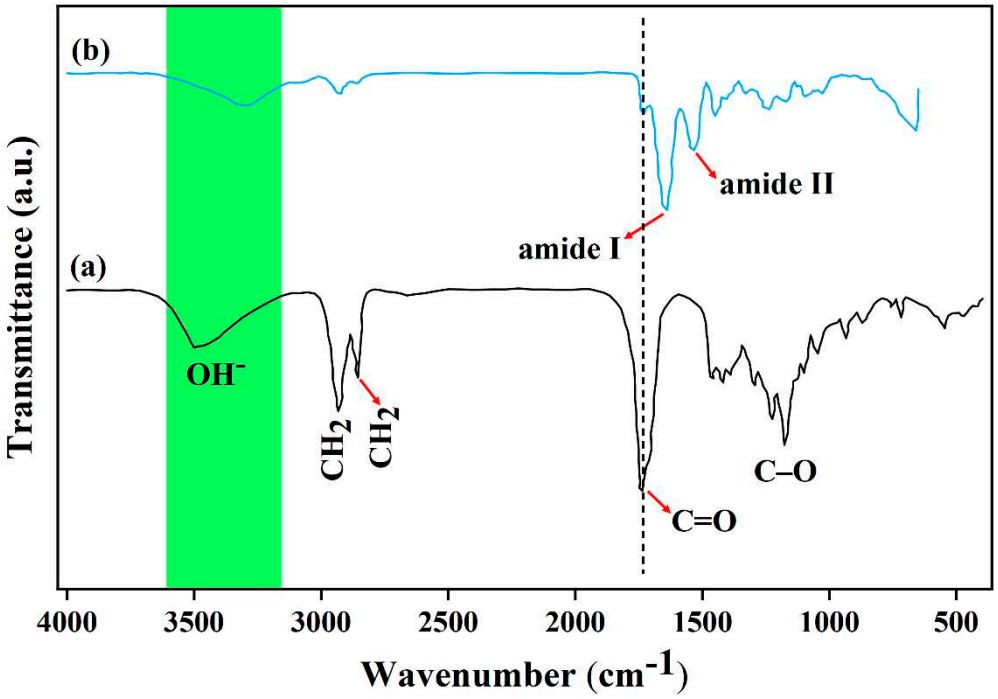

Figure 3. The FTIR spectra of (a) PGS and (b) PGS/Gel.

3.4. Hydrophilicity assessment

Contact angle measurements were used to evaluate the hydrophilicity of the scaffolds. Hydrophilic surfaces have contact angles below 90°, while hydrophobic ones show contact angles of above 90°. As shown in Figure 4, the contact angle of the scaffolds has decreased from 110.8° ± 4.3° to 54.9° ± 2.1° after adding gelatin, and the scaffolds became hydrophilic.

Preprints (www.preprints.org) | NOT PEER-REVIEWED | Posted: 8 May 2023 doi:10.20944/preprints202305.0451.v1

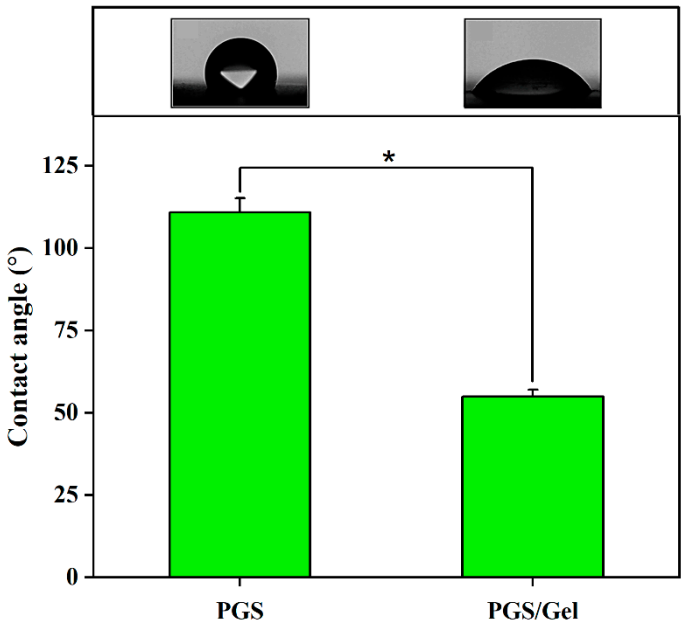

Figure 4. The water contact angle measurements of the samples.

3.5. In vitro degradation

Weight loss measurements were performed to evaluate the biodegradation behavior of the scaffolds. As indicated in Figure 5, the pure PGS scaffold has lost only 10.1 ± 4.2% of its weight over 21 days. The addition of gelatin increased the rate of biodegradation, and the weight loss of the scaffold reached 79.7 ± 3.4% of its initial weight during the same time.

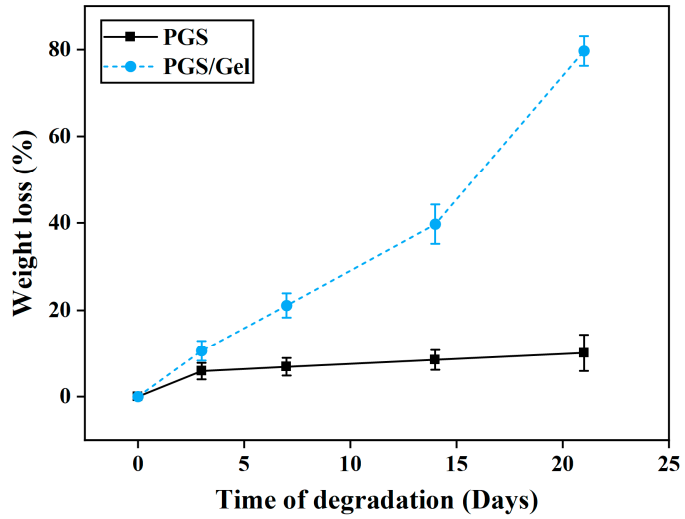

Figure 5. The weight loss measurements of the samples immersed in the PBS solution.

3.6. In vitro cellular studies

The MTT assay was applied to assess the cell viability of the scaffolds. Figure 6 shows that there is no significant ($p > 0.05$) difference between the viability of the cells cultured on the pure PGS and the control (scaffold-free) sample, while the PGS/Gel scaffold has significantly ($p < 0.05$) increased cell viability (compared to the control sample).

Preprints (www.preprints.org) | NOT PEER-REVIEWED | Posted: 8 May 2023 doi:10.20944/preprints202305.0451.v1

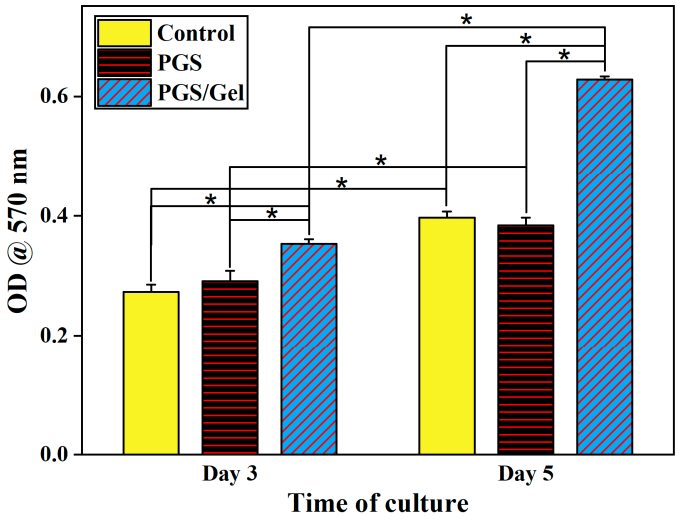

Figure 6. The MTT results of the samples.

Also, the SEM micrographs were taken on the 5th day of cell culture to observe cell attachment on the surface of the PGS/Gel scaffold (Figure 7). According to the results, the PGS/Gel scaffold has supported the attachment and spreading of the fibroblast cells.

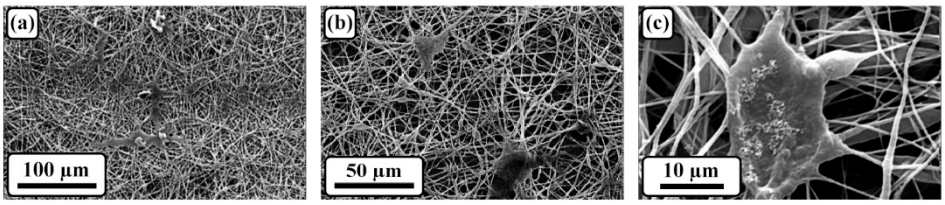

Figure 7. The SEM micrographs of the PGS/Gel scaffold on the 5th day of cell culture at (a) 250x, (b) 500x, and (c) 2000x magnifications.

4. Discussion

Fiber uniformity and integrity are among the main morphological factors of electrospun scaffold to provide an appropriate surface, promoting cell attachment and proliferation [33,34]. Adding gelatin has resulted in the production of a more uniform nanofibrous structure, possibly due to the hydrogen bonding between PGS and Gel [35], which has been further discussed below. Yang et al. confirmed the formation of hydrogen bonds between Gel and poly (3-hydroxybutyrate-co-4-hydroxybutyrate) (P3,4HB) polyester [36]. Another factor, porosity percentage, is important in scaffold designing. A porous 3D scaffold with a porosity percentage of above 70% has an interconnected structure, allowing the cells to penetrate in its depth as well as facilitating nutrient and waste exchange [37]. All the fabricated scaffolds have a porosity percentage above 75%, showing a suitable 3D structure which could be applied in biomedical applications. Based on FTIR results, the shift of the carbonyl functional group peak to lower wavenumbers and a decrease in its intensity could be attributed to the formation of hydrogen bonds between the carbonyl groups of PGS and amide groups of Gel. Other study showed that hydrogen bonds were formed between Gel and Polycaprolacton (PCl) electrospun multilayer nanofibrous scaffold [38].

Surface properties, such as hydrophilicity, should be optimized to promote cell attachment, spreading, and proliferation. Water contact angle measurement is a general technique to assess the hydrophilicity of the scaffolds' surface [33]. According to other studies [34,37], the surfaces with water contact angles in the range of 40°-80° have appropriate hydrophilicity and can support cell adhesion and proliferation. Based on the results, adding gelatin has significantly ($p < 0.05$) decreased the water contact angle of the PGS/Gel scaffold, probably due to its hydrophilic nature due to the presence of hydroxyl groups, which has been confirmed by other studies [39,40]. Also, the formation

of hydrogen bonds in the PGS/Gel scaffold (based on FTIR results) could be another reason for the increasing trend of the hydrophilicity of the scaffold, proved by another study [33].

The biodegradation rate of an ideal scaffold should be matched with the rate of the wound healing process [37]. Due to their high porosity and nano-sized fibers, electrospun structures possess relatively high surface area, making them suitable to be used as a biodegradable scaffold [34]. The results of in vitro biodegradation analysis show that the pure PGS scaffold has a very slow degradation rate over 21 days due to its hydrophobicity, which is not desirable for wound healing applications [41]. On the other hand, adding Gel increased the biodegradation rate of the PGS/Gel scaffold because of the Gel hydrophilic nature [38,42,43] and the formation of hydrogen bonding between Gel and PGS [34]. Also, the MTT results indicate that adding Gel has significantly ($p < 0.05$) increased viability of the cells cultured on the PGS/Gel scaffold, which could be attributed to the hydrophilic nature of Gel, the presence of sufficient hydroxyl groups on the surface of the scaffold [37], and the formation of hydrogen bonding interactions between PGS and Gel [34]. Wang et al. showed that the presence of Gel in the PCL/Gel hierarchical scaffolds caused an increment in the viability of the cultured cells on the blend scaffolds [44]. Moreover, confirming the MTT results, the SEM micrographs of the 5th day of cell culture show the appropriate cell attachment and proliferation on the surface of the PGS/Gel scaffolds. Other studies indicated a superior cellular behavior of the PGS/Gel scaffold, making it suitable for cardiac tissue engineering applications [27,45].

5. Conclusions

Here, the PGS/Gel nanofibrous scaffold was electrospun with optimal solution concentration and PGS-to-Gel ratio. The optimal PGS-to-Gel ratio and polymer concentration are 3:1 and 30 wt. %, respectively. The PGS/Gel scaffold was fabricated with uniform and continuous nanofibers using a voltage of 20 kV, a flow rate of 0.5 ml/h, and a needle-to-collector distance of 15 cm. SEM results show that the PGS/Gel scaffold has a uniform and porous nanofibrous structure with a fiber diameter of 252.4 ± 32.5 nm. The FTIR results indicate the possibility of the formation of hydrogen bonding between PGS and Gel. In addition, WCA measurements demonstrate that the PGS/Gel scaffold has a WCA of 54.9° ± 2.1°, showing the hydrophilicity of the blend scaffold. In vitro degradation results also show that adding Gel has optimized the rate of degradation. Moreover, MTT assay and cell attachment results indicate the positive effects of adding Gel on the biological properties of the blend scaffold. In conclusion, the results of this study could help biomedical engineers to design and fabricate a wound dressing with optimal properties.

Author Contributions: Conceptualization, M.N. and L.T.; methodology, M.N. and A.H.; investigation M.N. and A.H.; writing—original draft preparation M.N.; writing—review and editing, L.T.; supervision, L.T.; funding acquisition, L.T. All authors have read and agreed to the published version of the manuscript

Funding: L.T. acknowledges the partial support from National Institute of Dental & Craniofacial Research of the National Institutes of Health under award numbers R56 DE029191 and R15DE027533.

Data Availability Statement: There is no additional data available for this study other than what is reported in the manuscript.

Acknowledgments: The content is solely the responsibility of the authors and does not necessarily represent the official views of the National Institutes of Health. The figures are modified by Biorender.com.

Conflicts of Interest: The authors declare no conflict of interest.

References

1. Crowe, E.; Scott, C.; Cameron, S.; Cundell, J.H.; Davis, J. Developing Wound Moisture Sensors: Opportunities and Challenges for Laser-Induced Graphene-Based Materials. *J. Compos. Sci.* **2022**, *6*, doi:10.3390/jcs6060176.
2. Youssefi Azarfam, M.; Nasirinezhad, M.; Naeim, H.; Zarrintaj, P.; Saeb, M. A Green Composite Based on Gelatin/Agarose/Zeolite as a Potential Scaffold for Tissue Engineering Applications. *J. Compos. Sci.* **2021**, *5*, doi:10.3390/jcs5050125.

3. Jales, S.T.L.; Barbosa, R.d.M.; de Albuquerque, A.C.; Duarte, L.H.V.; da Silva, G.R.; Meirelles, L.M.A.; da Silva, T.M.S.; Alves, A.F.; Viseras, C.; Raffin, F.N.; et al. Development and Characterization of *Aloe vera* Mucilaginous-Based Hydrogels for Psoriasis Treatment. *J. Compos. Sci.* **2022**, *6*, doi:10.3390/jcs6080231.
4. Yao, Z.; Xu, J.; Shen, J.; Qin, L.; Yuan, W. Biomimetic Hierarchical Nanocomposite Hydrogels: From Design to Biomedical Applications. *J. Compos. Sci.* **2022**, *6*, doi:10.3390/jcs611034.
5. Rokaya, D.; Skallevold, H.E.; Srimaneepong, V.; Marya, A.; Shah, P.K.; Khurshid, Z.; Zafar, M.S.; Sapkota, J. Shape Memory Polymeric Materials for Biomedical Applications: An Update. *J. Compos. Sci.* **2023**, *7*, doi:10.3390/jcs7010024.
6. Vizely, K.; Wagner, K.T.; Mandla, S.; Gustafson, D.; Fish, J.E.; Radisic, M. Angiopoietin-1 derived peptide hydrogel promotes molecular hallmarks of regeneration and wound healing in dermal fibroblasts. *iSci.* **2023**, *26*, 105984, doi:https://doi.org/10.1016/j.isci.2023.105984.
7. Hu, W.; Yu, H.; Zhou, X.; Li, M.; Xiao, L.; Ruan, Q.; Huang, X.; Li, L.; Xie, W.; Guo, X.; et al. Topical administration of pterostilbene accelerates burn wound healing in diabetes through activation of the HIF1α signaling pathway. *Burn.* **2022**, *48*, 1452-1461, doi:https://doi.org/10.1016/j.burns.2021.10.019.
8. Priyadarshi, A.; Keshri, G.K.; Gupta, A. *Hippophae rhamnoides L.* leaf extract diminishes oxidative stress, inflammation and ameliorates bioenergetic activation in full-thickness burn wound healing. *Phytomed. Plus* **2022**, *2*, 100292, doi:https://doi.org/10.1016/j.phyplu.2022.100292.
9. de Lacerda Bukzem, A.; dos Santos, D.M.; Leite, I.S.; Inada, N.M.; Campana-Filho, S.P. Tuning the properties of carboxymethylchitosan-based porous membranes for potential application as wound dressing. *Int. J. Biol. Macromol.* **2021**, *166*, 459-470, doi:https://doi.org/10.1016/j.ijbiomac.2020.10.204.
10. Wu, G.; Ma, X.; Fan, L.; Gao, Y.; Deng, H.; Wang, Y. Accelerating dermal wound healing and mitigating excessive scar formation using LBL modified nanofibrous mats. *Mater. Des.* **2020**, *185*, 108265, doi:https://doi.org/10.1016/j.matdes.2019.108265.
11. Liu, N.; Zhu, S.; Deng, Y.; Xie, M.; Zhao, M.; Sun, T.; Yu, C.; Zhong, Y.; Guo, R.; Cheng, K.; et al. Construction of multifunctional hydrogel with metal-polyphenol capsules for infected full-thickness skin wound healing. *Bioact. Mater.* **2023**, *24*, 69-80, doi:https://doi.org/10.1016/j.bioactmat.2022.12.009.
12. Kalaycıoğlu, Z.; Kahya, N.; Adımcılar, V.; Kaygusuz, H.; Torlak, E.; Akın-Evingür, G.; Erim, F.B. Antibacterial nano cerium oxide/chitosan/cellulose acetate composite films as potential wound dressing. *Eur. Polym. J.* **2020**, *133*, 109777, doi:https://doi.org/10.1016/j.eurpolymj.2020.109777.
13. Poonguzhali, R.; Khaleel Basha, S.; Sugantha Kumari, V. Novel asymmetric chitosan/PVP/nanocellulose wound dressing: In vitro and in vivo evaluation. *Int. J. Biol. Macromol.* **2018**, *112*, 1300-1309, doi:https://doi.org/10.1016/j.ijbiomac.2018.02.073.
14. Soubhagya, A.S.; Moorthi, A.; Prabaharan, M. Preparation and characterization of chitosan/pectin/ZnO porous films for wound healing. *Int. J. Biol. Macromol.* **2020**, *157*, 135-145, doi:https://doi.org/10.1016/j.ijbiomac.2020.04.156.
15. Yang, J.; Wang, K.; Yu, D.-G.; Yang, Y.; Bligh, S.W.A.; Williams, G.R. Electrospun Janus nanofibers loaded with a drug and inorganic nanoparticles as an effective antibacterial wound dressing. *Mater. Sci. Eng.: C* **2020**, *111*, 110805, doi:https://doi.org/10.1016/j.msec.2020.110805.
16. Chen, K.; Pan, H.; Ji, D.; Li, Y.; Duan, H.; Pan, W. Curcumin-loaded sandwich-like nanofibrous membrane prepared by electrospinning technology as wound dressing for accelerate wound healing. *Mater. Sci. Eng.: C* **2021**, *127*, 112245, doi:https://doi.org/10.1016/j.msec.2021.112245.
17. Mistry, P.; Chhabra, R.; Muke, S.; Narvekar, A.; Sathaye, S.; Jain, R.; Dandekar, P. Fabrication and characterization of starch-TPU based nanofibers for wound healing applications. *Mater. Sci. Eng.: C* **2021**, *119*, 111316, doi:https://doi.org/10.1016/j.msec.2020.111316.
18. Rodríguez-Tobías, H.; Morales, G.; Grande, D. Comprehensive review on electrospinning techniques as versatile approaches toward antimicrobial biopolymeric composite fibers. *Mater. Sci. Eng.: C* **2019**, *101*, 306-322, doi:https://doi.org/10.1016/j.msec.2019.03.099.
19. Hadizadeh, M.; Naeimi, M.; Rafienia, M.; Karkhaneh, A. A bifunctional electrospun nanocomposite wound dressing containing surfactin and curcumin: In vitro and in vivo studies. *Mater. Sci. Eng.: C* **2021**, *129*, 112362, doi:https://doi.org/10.1016/j.msec.2021.112362.
20. Bao, X.; Zhu, Q.; Chen, Y.; Tang, H.; Deng, W.; Guo, H.; Zeng, L. Antibacterial and antioxidant films based on HA/Gr/TA fabricated using electrospinning for wound healing. *Int. J. Pharm.* **2022**, *626*, 122139, doi:https://doi.org/10.1016/j.ijpharm.2022.122139.

21. Heydari, P.; Zargar Kharazi, A.; Asgary, S.; Parham, S. Comparing the wound healing effect of a controlled release wound dressing containing curcumin/ciprofloxacin and simvastatin/ciprofloxacin in a rat model: A preclinical study. *J. Biomed. Mater. Res. Part A* **2022**, *110*, 341-352, doi:https://doi.org/10.1002/jbm.a.37292.
22. Yang, X.; Li, L.; Yang, D.; Nie, J.; Ma, G. Electrospun Core–Shell Fibrous 2D Scaffold with Biocompatible Poly(Glycerol Sebacate) and Poly-l-Lactic Acid for Wound Healing. *Adv. Fiber Mater.* **2020**, *2*, 105-117, doi:10.1007/s42765-020-00027-x.
23. Khaloo Kermani, P.; Zargar Kharazi, A. A Promising Antibacterial Wound Dressing Made of Electrospun Poly (Glycerol Sebacate) (PGS)/Gelatin with Local Delivery of Ascorbic Acid and Pantothenic Acid. *J. Polym. Environ.* **2022**, doi:10.1007/s10924-022-02715-8.
24. Jafari, A.; Amirsadeghi, A.; Hassanajili, S.; Azarpira, N. Bioactive antibacterial bilayer PCL/gelatin nanofibrous scaffold promotes full-thickness wound healing. *Int. J. pharm.* **2020**, *583*, 119413, doi:https://doi.org/10.1016/j.ijpharm.2020.119413.
25. Sanhueza, C.; Hermosilla, J.; Bugallo-Casal, A.; Da Silva-Candal, A.; Taboada, C.; Millán, R.; Concheiro, A.; Alvarez-Lorenzo, C.; Acevedo, F. One-step electrospun scaffold of dual-sized gelatin/poly-3-hydroxybutyrate nano/microfibers for skin regeneration in diabetic wound. *Mater. Sci. Eng.: C* **2021**, *119*, 111602, doi:https://doi.org/10.1016/j.msec.2020.111602.
26. Farahani, H.; Barati, A.; Arjomandzadegan, M.; Vatankhah, E. Nanofibrous cellulose acetate/gelatin wound dressing endowed with antibacterial and healing efficacy using nanoemulsion of *Zataria multiflora*. *Int. J. Biol. Macromol.* **2020**, *162*, 762-773, doi:https://doi.org/10.1016/j.ijbiomac.2020.06.175.
27. Kharaziha, M.; Nikkhah, M.; Shin, S.-R.; Annabi, N.; Masoumi, N.; Gaharwar, A.K.; Camci-Unal, G.; Khademhosseini, A. PGS:Gelatin nanofibrous scaffolds with tunable mechanical and structural properties for engineering cardiac tissues. *Biomater.* **2013**, *34*, 6355-6366, doi:https://doi.org/10.1016/j.biomaterials.2013.04.045.
28. Movahedi, M.; Karbasi, S. Electrospun halloysite nanotube loaded polyhydroxybutyrate-starch fibers for cartilage tissue engineering. *Int. J. Biol. Macromol.* **2022**, *214*, 301-311, doi:https://doi.org/10.1016/j.ijbiomac.2022.06.072.
29. Ghasemi-Mobarakeh, L.; Semnani, D.; Morshed, M. A novel method for porosity measurement of various surface layers of nanofibers mat using image analysis for tissue engineering applications. *J. Appl. Polym. Sci.* **2007**, *106*, 2536-2542, doi:https://doi.org/10.1002/app.26949.
30. Rostamian, M.; Kalaee, M.R.; Dehkordi, S.R.; Panahi-Sarmad, M.; Tirgar, M.; Goodarzi, V. Design and characterization of poly(glycerol-sebacate)-co-poly(caprolactone) (PGS-co-PCL) and its nanocomposites as novel biomaterials: The promising candidate for soft tissue engineering. *Eur. Polym. J.* **2020**, *138*, 109985, doi:https://doi.org/10.1016/j.eurpolymj.2020.109985.
31. Gultekinoglu, M.; Öztürk, Ş.; Chen, B.; Edirisinghe, M.; Ulubayram, K. Preparation of poly(glycerol sebacate) fibers for tissue engineering applications. *Eur. Polym. J.* **2019**, *121*, 109297, doi:https://doi.org/10.1016/j.eurpolymj.2019.109297.
32. Aghajan, M.H.; Panahi-Sarmad, M.; Alikarami, N.; Shojaei, S.; Saeidi, A.; Khonakdar, H.A.; Shahrousvan, M.; Goodarzi, V. Using solvent-free approach for preparing innovative biopolymer nanocomposites based on PGS/gelatin. *Eur. Polym. J.* **2020**, *131*, 109720, doi:https://doi.org/10.1016/j.eurpolymj.2020.109720.
33. Sarrami, P.; Karbasi, S.; Farahbakhsh, Z.; Bigham, A.; Rafienia, M. Fabrication and characterization of novel polyhydroxybutyrate-keratin/nanohydroxyapatite electrospun fibers for bone tissue engineering applications. *Int. J. Biol. Macromol.* **2022**, *220*, 1368-1389, doi:https://doi.org/10.1016/j.ijbiomac.2022.09.117.
34. Asl, M.A.; Karbasi, S.; Beigi-Boroujeni, S.; Zamanlui Benisi, S.; Saeed, M. Evaluation of the effects of starch on polyhydroxybutyrate electrospun scaffolds for bone tissue engineering applications. *Int. J. Biol. Macromol.* **2021**, *191*, 500-513, doi:https://doi.org/10.1016/j.ijbiomac.2021.09.078.
35. El Fawal, G.; Hong, H.; Mo, X.; Wang, H. Fabrication of scaffold based on gelatin and polycaprolactone (PCL) for wound dressing application. *J. Drug Deliv. Sci. Technol.* **2021**, *63*, 102501, doi:https://doi.org/10.1016/j.jddst.2021.102501.
36. Yang, Q.; Guo, J.; Liu, Y.; Guan, F.; Sun, F.; Gong, X. Preparation and characterization of poly(3-hydroxybutyrate-co-4-hydroxybutyrate)/gelatin composite nanofibrous. *Surf. Interface.* **2022**, *33*, 102231, doi:https://doi.org/10.1016/j.surfin.2022.102231.
37. Mohammadalipour, M.; Behzad, T.; Karbasi, S.; Mohammadalipour, Z. Optimization and characterization of polyhydroxybutyrate/lignin electro-spun scaffolds for tissue engineering applications. *Int. J. Biol. Macromol.* **2022**, *218*, 317-334, doi:https://doi.org/10.1016/j.ijbiomac.2022.07.139.

38. Hedayatnazari, A., M. Movahedi, and M. Naseri, *Fabrication And Characterization Of Bilayer Wound Dressing Polyurethane-Gelatin/Polycaprolactone For Usage In Tissue Engineering.* **2021**.
39. Liu, W.; Zhang, M.; Zhou, M.; Gu, C.; Ye, Z.; Xiao, Y.; Zhou, Y.; Lang, M.; Tan, W.-S. Fabrication and evaluation of modified poly(ethylene terephthalate) microfibrous scaffolds for hepatocyte growth and functionality maintenance. *Mater. Sci. Eng.: C* **2020**, *109*, 110523, doi:https://doi.org/10.1016/j.msec.2019.110523.
40. Pozzobon, L.G.; Sperling, L.E.; Teixeira, C.E.; Malysz, T.; Pranke, P. Development of a conduit of PLGA-gelatin aligned nanofibers produced by electrospinning for peripheral nerve regeneration. *Chem-Biol. Interact.* **2021**, *348*, 109621, doi:https://doi.org/10.1016/j.cbi.2021.109621.
41. Saudi, A.; Amini, S.; Amirpour, N.; Kazemi, M.; Zargar Kharazi, A.; Salehi, H.; Rafienia, M. Promoting neural cell proliferation and differentiation by incorporating lignin into electrospun poly(vinyl alcohol) and poly(glycerol sebacate) fibers. *Mater. Sci. Eng.: C* **2019**, *104*, 110005, doi:https://doi.org/10.1016/j.msec.2019.110005.
42. Rarima, R.; Unnikrishnan, G. Poly(lactic acid)/gelatin foams by non-solvent induced phase separation for biomedical applications. *Polym. Degrad. Stab.* **2020**, *177*, 109187, doi:https://doi.org/10.1016/j.polymdegradstab.2020.109187.
43. Nagiah, N.; Madhavi, L.; Anitha, R.; Anandan, C.; Srinivasan, N.T.; Sivagnanam, U.T. Development and characterization of coaxially electrospun gelatin coated poly (3-hydroxybutyric acid) thin films as potential scaffolds for skin regeneration. *Mater. Sci. Eng.: C* **2013**, *33*, 4444-4452, doi:https://doi.org/10.1016/j.msec.2013.06.042.
44. Wang, Z.; Wang, H.; Xiong, J. ;Li, J.; Miao, X.; Lan, X.; Liu, X.; Wang, W.; Cai, N.; Tang, Y. Fabrication and in vitro evaluation of PCL/gelatin hierarchical scaffolds based on melt electrospinning writing and solution electrospinning for bone regeneration. *Mater. Sci. Eng.: C* **2021**, *128*, 112287, doi:https://doi.org/10.1016/j.msec.2021.112287.
45. Masoumi, N.; Jean, A.; Zugates, J.T.; Johnson, K.L.; Engelmayr Jr, G.C. Laser microfabricated poly(glycerol sebacate) scaffolds for heart valve tissue engineering. *J. Biomed. Mater. Res. Part A* **2013**, *101A*, 104-114, doi:https://doi.org/10.1002/jbm.a.34305.